

HI Fluctuations at Large Redshifts: I–Visibility correlation

Somnath Bharadwaj

*Department of Physics and Meteorology & Center for Theoretical Studies,
I.I.T. Kharagpur, 721 302, India*

`somnath@phy.iitkgp.ernet.in`

and

Shiv K. Sethi

Harish-Chandra Research Institute, Chhatnag Road, Jhusi, Allahabad 211 019, India

`sethi@mri.ernet.in`

ABSTRACT

We investigate the possibility of probing the large scale structure in the universe at large redshifts by studying fluctuations in the redshifted 1420 MHz emission from the neutral hydrogen (HI) at early epochs. The neutral hydrogen content of the universe is known from absorption studies for $z \lesssim 4.5$. The HI distribution is expected to be inhomogeneous in the gravitational instability picture and this inhomogeneity leads to anisotropy in the redshifted HI emission. The best hope of detecting this anisotropy is by using a large low-frequency interferometric instrument like the Giant Meter-Wave Radio Telescope (GMRT). We calculate the visibility correlation function $\langle V_\nu(\mathbf{U})V_{\nu'}(\mathbf{U}) \rangle$ at two frequencies ν and ν' of the redshifted HI emission for an interferometric observation. In particular we give numerical results for the two GMRT channels centered around $\nu = 325$ MHz and $\nu = 610$ MHz from density inhomogeneity and peculiar velocity of the HI distribution. The visibility correlation is $\simeq 10^{-10}$ – 10^{-9} Jy 2 . We calculate the signal-to-noise for detecting the correlation signal in the presence of system noise and show that the GMRT might detect the signal for integration times $\simeq 100$ hrs. We argue that the measurement of visibility correlation allows optimal use of the uncorrelated nature of the system noise across baselines and frequency channels.

Subject headings: cosmology:theory, observations, large scale structures - diffuse radiation.

1. Introduction

Various observations indicate that around 90% of the HI mass in the redshift range 2 to 3.5 is in clouds which have HI column densities greater than 2×10^{20} atoms/cm 2 (Peroux *et al.*

2001, Storrie-Lombardi, McMahon, Irwin 1996, Lanzetta, Wolfe, & Turnshek 1995). These high column density clouds are responsible for the damped Lyman- α absorption lines observed along lines of sight to quasars. The flux of HI emission from individual clouds ($\lesssim 10\mu\text{Jy}$) is too weak to be detected by existing radio telescopes unless the image of the cloud is significantly magnified by an intervening cluster gravitational lens (Saini, Bharadwaj and Sethi, 2001). Although we may not be able to detect individual clouds, the redshifted HI emission from the distribution of clouds will appear as background radiation in low frequency radio observations. Bharadwaj, Nath and Sethi (2001; hereafter referred to as BNS) have used existing estimates of the HI density at $z \simeq 3$ to infer the mean brightness temperature of $\simeq 1\text{ mK}$ at $\nu \simeq 320\text{ MHz}$ for this radiation. The fluctuations in the brightness temperature of this radiation arise from fluctuations in the HI number density and from peculiar velocities. As shown in BNS, the cross-correlation between the temperature fluctuations across different frequencies and different lines of sight is related to the two-point correlation function (or equivalently the power spectrum) of density perturbations at the redshift where the radiation originates. The possibility of measuring this provides a new method for studying large scale structures at high redshifts. Estimates indicate the expected values of the cross-correlations in the brightness temperature to vary from 10^{-7} K^2 to 10^{-8} K^2 over intervals corresponding to spatial scales from 10 Mpc to 40 Mpc for some of the currently-favoured cosmological models. Estimates of the different contributions to the flux expected in a pixel of a radio image show the contribution from galactic and extragalactic sources and the system noise to be substantially higher than the contribution from the HI radiation. The task of devising a strategy for extracting the signal from the various foregrounds and noise in which it is buried is a problem which has still to be solved. A possible strategy based on the very distinct spectral properties of the foregrounds as against the HI emission is discussed in BNS.

An alternate strategy for using the HI emission from high redshifts to study large scale structures has been discussed by many authors (Subramanian & Padmanabhan 1993, Kumar, Padmanabhan & Subramanian, Bagla, Nath, & Padmanabhan, Bagla 1998). This is based on detecting the HI emission from individual protoclusters at high redshifts. There have also been observational efforts in this direction (see Subrahmanyam & Anantharamaiah 1990 and reference therein). No detections have been made till date. This strategy suffers from the disadvantage that the protoclusters correspond to very large overdense regions which are very rare events. Protoclusters with flux in the range 3 to 5 mJy are predicted to occur with abundances in the range $10^{-8} - 10^{-7}\text{ Mpc}^{-3}$ in the CDM model (Subramanian and Padmanabhan, 1993). In the statistical approach proposed in BNS fluctuations of all magnitude in the HI distribution contribute to the signal. The statistical approach allows optimum use of the signal present in all the pixels of the images made at different frequencies across the bandwidth of a typical radio observation. In this paper we take up various issues related to the statistical approach originally proposed in BNS.

The main focus of this paper is the choice of an appropriate statistical estimator to quantify the properties of the signal and the system noise. The statistical estimator proposed in BNS is the cross-correlation between the temperature fluctuations along different lines of sight in radio map

made at different frequencies. While this quantity is conceptually very simple, complications arise when it is applied to images produced by radio interferometry, as is the case with most low frequency radio telescopes. Such observations measure the coherence between the signals arriving at any two antennas, a quantity known as the visibility $V(\mathbf{U})$. This is measured for all pairs of antennas in the interferometric array. Here \mathbf{U} refers to the vector joining a pair of antennas, measured in units of λ , projected on the plane perpendicular to the direction which is being imaged.

The image is produced by a Fourier transform of the visibility

$$I_\nu(\vec{\theta}) = \int V(\mathbf{U}) \exp[2\pi i \vec{\theta} \cdot \mathbf{U}] d^2 \mathbf{U} \quad (1)$$

where $\vec{\theta}$ refers to different positions in the small patch of the sky which is being imaged, and $I_\nu(\vec{\theta})$ is the specific intensity. The contribution of system noise to the signal from each antenna is independent, and the visibilities measured by each pair of antennas are uncorrelated. The noise in the pixels of a radio image constructed from the visibilities is not independent. The correlations in the noise in the pixels depend on the detailed distribution of the different separations (baselines) \mathbf{U} for which the visibility has been measured. Any strategy based on the statistical analysis of radio images will be faced with the problem of distinguishing the correlations in fluctuations of the HI emission from the correlations in the noise. This complication can be avoided by dealing directly with the visibilities. In this paper we investigate the possibility of detecting the fluctuations in the HI emission using a statistical estimator constructed directly from the visibilities measured in a radio interferometric observation, without making an image.

We next present a brief outline of this paper. In section 2 we calculate the relation between the statistical properties of the HI fluctuations and the visibilities produced by these fluctuations. In Section 3 we present numerical estimates of these quantities for some of the currently favoured cosmological models for the system parameters of GMRT (Swarup *et al.* 1990). In Section 4, we calculate statistical properties of the visibility correlations arising from the system noise. In Section 5 we present the conclusions and discuss possible directions for future work.

2. From Density Fluctuations to Visibility

We consider radio-interferometric observations of a small patch of the sky whose center is in the direction of the unit vector \mathbf{n} (Figure 1). A small patch of the sky may be treated as a plane, and the angle $\vec{\theta}$ which refers to different directions in the sky (Figure 1) may be treated as a two dimensional vector. Observations at a frequency ν would measure the HI emission from a redshift $z = (1420 \text{ MHz}/\nu) - 1$ or equivalently a comoving distance r_ν . The specific intensity of the redshifted HI emission arriving from any direction $\vec{\theta}$ may be decomposed into two parts

$$I_\nu(\vec{\theta}) = \bar{I}_\nu + \Delta I_\nu(\vec{\theta}), \quad (2)$$

where \bar{I}_ν and $\Delta I_\nu(\mathbf{n})$ are the isotropic and the fluctuating components of the specific intensity. The isotropic component \bar{I}_ν is related to $\bar{n}_{\text{HI}}(z)$, the mean comoving number density of HI atoms in the

excited state at a redshift z and we have

$$\bar{I}_\nu = \frac{A_{21} h_P c \bar{n}_{\text{HI}}(z)}{4\pi H(z)} \quad (3)$$

where A_{21} is the Einstein coefficient for the HI hyperfine transition, h_P the Plank constant, c the speed of light and $H(z)$ the Hubble parameter. This is a slightly rearranged version of Equation (11) of BNS.

The fluctuations in the specific intensity $\Delta I_\nu(\vec{\theta})$ arise from fluctuations in the HI number density $\Delta n_{\text{HI}}(\mathbf{x})$ and the peculiar velocity $\mathbf{v}(\mathbf{x})$, where \mathbf{x} refers to the comoving position $\mathbf{x} = r_\nu(\mathbf{n} + \vec{\theta})$. The details of the calculation relating these quantities are presented in BNS, and we use a slightly rearranged version of Equation (12) of BNS

$$\Delta I_\nu(\vec{\theta}) = \bar{I}_\nu \left[\frac{\Delta n_{\text{HI}}(\mathbf{x})}{\bar{n}_{\text{HI}}} + \frac{(\mathbf{n} \cdot \nabla)(\mathbf{n} \cdot \mathbf{v}(\mathbf{x}))}{aH} \right] \quad (4)$$

where a is the scale factor. It should be noted that all the quantities in the right hand side of equation (4) should be evaluated at the epoch when the radiation was emitted.

In this paper we wish to calculate the contribution from the redshifted HI emission to the visibilities $V_\nu(\mathbf{U})$ that would be measured in radio-interferometric observations. The relation between the specific intensity and the visibilities is

$$V_\nu(\mathbf{U}) = \int d^2\theta A(\vec{\theta}) \Delta I_\nu(\vec{\theta}) e^{-i2\pi\mathbf{U}\cdot\vec{\theta}}. \quad (5)$$

Only the fluctuating part of the specific intensity contributes to the visibility, and we have dropped the isotropic component from eq. (5). Here $A(\vec{\theta})$ is the beam pattern of the individual antennas in the array (primary beam). We use equations (4) and (5) to relate the visibilities to the fluctuations in the HI distribution.

It is convenient to work with $\Delta_{\text{HI}}(\mathbf{k})$, the Fourier transform of the density contrast of the HI number density $\Delta n_{\text{HI}}(\mathbf{x})/\bar{n}_{\text{HI}}$. We assume that on sufficiently large scales $\Delta_{\text{HI}}(\mathbf{k})$ can be related to $\Delta(\mathbf{k})$, the density contrast of the underlying dark matter distribution, through a linear bias parameter b i.e. $\Delta_{\text{HI}}(\mathbf{k}) = b_{\text{HI}}\Delta(\mathbf{k})$. We also assume that the scales we are dealing with are sufficiently large that we can apply linear theory of density perturbations (Peebles 1980) to relate the peculiar velocities to the fluctuations in the dark matter distribution, $\mathbf{v}(\mathbf{k}) = (-iaHf(\Omega_m)\mathbf{k}/k)\Delta(\mathbf{k})$, where $f(\Omega_m) \approx \Omega_m^{0.6} + \frac{1}{70}[1 - \frac{1}{2}\Omega_m(1 + \Omega_m)]$ in a spatially flat universe (Lahav *et al.* 1991). These assumptions allow us to express the fluctuations in the specific intensity as

$$\Delta I_\nu(\vec{\theta}) = \bar{I}_\nu \int \frac{d^3k}{(2\pi)^3} \left[1 + \frac{\beta k_\parallel^2}{k^2} \right] \Delta_{\text{HI}}(\mathbf{k}) e^{ir_\nu(k_\parallel + \mathbf{k}_\perp \cdot \vec{\theta})} \quad (6)$$

where we have decomposed the wave vector \mathbf{k} into two parts $\mathbf{k} = k_\parallel \mathbf{n} + \mathbf{k}_\perp$ where $k_\parallel \mathbf{n}$ refers to the component of the Fourier mode \mathbf{k} along the line of sight to the center of the patch of sky

being observed, and \mathbf{k}_\perp refers to the component of \mathbf{k} in the plane of the sky. We use equation (6) in equation (5) to express the visibility $V_\nu(\mathbf{U})$ in terms of $\Delta(\mathbf{k})$. This allows us to carry out the integral over $\vec{\theta}$ which gives us

$$V_\nu(u, v) = \bar{I}_\nu \int \frac{d^3 k}{(2\pi)^3} \Delta_{\text{HI}}(\mathbf{k}) \left[1 + \frac{\beta k_\parallel^2}{k^2} \right] e^{i r_\nu k_\parallel} a(\mathbf{U} - \frac{\mathbf{k}_\perp r_\nu}{2\pi}) \quad (7)$$

where $a(\mathbf{U})$ is the Fourier transform of $A(\vec{\theta})$ the primary beam,

$$a(\mathbf{U}) = \int d^2 \vec{\theta} A(\vec{\theta}) e^{-i 2\pi \mathbf{U} \cdot \vec{\theta}}. \quad (8)$$

For a Gaussian primary beam pattern $A(\theta) = e^{-\theta^2/\theta_0^2}$. the Fourier transform also is a Gaussian and we have

$$a(\mathbf{U}) = \pi \theta_0^2 \exp [-\pi^2 \theta_0^2 U^2] \quad (9)$$

which we use in the rest of this paper.

Equation (7) relates the contribution to the visibilities from fluctuations in the HI number density. These fluctuations are assumed to be a Gaussian random field, or equivalently the different modes $\Delta_{\text{HI}}(\mathbf{k})$ have independent, random phases. This allows us to predict all the statistical properties of $\Delta_{\text{HI}}(\mathbf{k})$ in terms of the power spectrum of the fluctuations in the HI distribution $P_{\text{HI}}(\mathbf{k})$ which is defined as $\langle \Delta_{\text{HI}}^*(\mathbf{k}) \Delta_{\text{HI}}(\mathbf{k}') \rangle = (2\pi)^3 \delta^3(\mathbf{k} - \mathbf{k}') P_{\text{HI}}(\mathbf{k})$ where $\langle \rangle$ denotes ensemble average. We use this to calculate the correlation between the visibilities at different baselines \mathbf{U} and \mathbf{U}' and two different frequencies ν and $\nu + \Delta\nu$. Here we assume that the bandwidth over which the observations are being carried out is small compared to the central frequency *i.e.* $\Delta\nu \ll \nu$ and $r_{\nu + \Delta\nu} = r_\nu + r'_\nu \Delta\nu$ where $r'_\nu = \frac{dr_\nu}{d\nu}$. Using these inputs to calculate the visibility correlation function we obtain

$$\begin{aligned} \langle V_\nu(\mathbf{U}) V_{\nu + \Delta\nu}^*(\mathbf{U}') \rangle &= [\bar{I}_\nu \theta_0^2 \pi]^2 \int \frac{d^3 k}{(2\pi)^3} P_{\text{HI}}(k) e^{i k_\parallel r'_\nu \Delta\nu} \left[1 + \beta \frac{k_\parallel^2}{k^2} \right]^2 \times \\ &\times \exp \left[-\frac{(\mathbf{k}_\perp - 2\pi \mathbf{U}/r_\nu)^2 + (\mathbf{k}_\perp - 2\pi \mathbf{U}'/r_\nu)^2}{(2/r_\nu \theta_0)^2} \right] \end{aligned} \quad (10)$$

The assumption of linear bias allows us to relate $P_{\text{HI}}(\mathbf{k})$ to $P(\mathbf{k})$ the power spectrum of density fluctuations in the dark matter distribution through the linear bias parameter $P_{\text{HI}}(\mathbf{k}) = b^2 P(\mathbf{k})$. We use this in later sections to obtain numerical estimates for different cosmological models.

We next turn our attention to a qualitative analysis of equation (10) to determine the nature and extent of the correlations between the visibilities measured at different baselines. This is largely governed by term $\exp \left[-\frac{(\mathbf{k}_\perp - 2\pi \mathbf{U}/r_\nu)^2 + (\mathbf{k}_\perp - 2\pi \mathbf{U}'/r_\nu)^2}{(2/r_\nu \theta_0)^2} \right]$ which arises because the observations have a limited sky coverage determined by the primary beam pattern. This term is very small for all values of \mathbf{k}_\perp unless $|\mathbf{U} - \mathbf{U}'| < 1/\theta_0$. The parameter θ_0 is related to the the FWHM of

the primary beam and $\theta_0 \approx 0.6\theta_{\text{FWHM}}$, which allows us to relate θ_0 to D the diameter of the individual antennas as $\theta_0 \approx \lambda/D$. We also express \mathbf{U} and \mathbf{U}' in terms of \mathbf{d} and \mathbf{d}' , the physical separations between the pairs of antennas as $\mathbf{U} = \mathbf{d}/\lambda$ and $\mathbf{U}' = \mathbf{d}'/\lambda'$. It should be noted that here and throughout we assume that $\lambda' = \lambda(1 - \Delta\nu/\nu)$ with $\Delta\nu \ll \nu$. Using these we see that the condition for the visibilities to be correlated can be expressed as $|\mathbf{d} - \mathbf{d}'| < D$. This implies that the visibilities measured by a pair of antennas separated by the displacement \mathbf{d} will be correlated to the visibilities measured by another pair separated by a displacement \mathbf{d}' only if difference in the two displacements \mathbf{d} and \mathbf{d}' is less than the antenna diameter. The consequences of this for a typical antenna configuration are

- (a) The visibilities measured at various frequencies by the same pair of antennas are correlated.
- (b) The visibilities measured by different pairs of antennas are uncorrelated.

For the rest of the paper we shall consider only the correlation between the visibilities measured at various frequencies by the same pair of antennas. We use the notation $\langle V_\nu(\mathbf{U})V_{\nu+\Delta\nu}^*(\mathbf{U}) \rangle$ to denote the correlation between the visibilities measured at two different frequencies by the pair of antennas at a physical separation $\mathbf{d} = c\mathbf{U}/\nu$. The fact that this physical separation \mathbf{d} will correspond to a different baseline $\mathbf{U}' = (\nu + \Delta\nu)\mathbf{d}/c$ at the frequency $\nu + \Delta\nu$ is ignored throughout as $\Delta\nu \ll \nu$. Equation (10) can now be used to obtain

$$\begin{aligned} \langle V_\nu(\mathbf{U})V_{\nu+\Delta\nu}^*(\mathbf{U}) \rangle &= [\bar{I}_\nu \theta_0^2 \pi]^2 \int \frac{d^3 k}{(2\pi)^3} P_{\text{HI}}(k) e^{ik_\parallel r'_\nu \Delta\nu} \left[1 + \beta \frac{k_\parallel^2}{k^2} \right]^2 \times \\ &\quad \times \exp \left[-\frac{(\mathbf{k}_\perp - 2\pi\mathbf{U}/r_\nu)^2}{2(1/r_\nu \theta_0)^2} \right] \end{aligned} \quad (11)$$

The role of the Gaussian in equation (11) arising from the primary beam pattern is to ensure that most of the contribution is from Fourier modes for which $\mathbf{k}_\perp \approx (2\pi/r_\nu)\mathbf{U}$. Equation (11) is further simplified if we approximate the Gaussian with a Dirac Delta function

$$\exp \left[-\frac{(\mathbf{k}_\perp - 2\pi\mathbf{U}/r_\nu)^2}{2(1/r_\nu \theta_0)^2} \right] \approx \frac{2\pi}{r_\nu^2 \theta_0^2} \delta^2 \left(\mathbf{k}_\perp - \frac{2\pi}{r_\nu} \mathbf{U} \right) \quad (12)$$

whereby only Fourier modes for which $\mathbf{k}_\perp = (2\pi/r_\nu)\mathbf{U}$ contribute. This allows us to do two of the integrals in equation (11) giving us

$$\begin{aligned} \langle V_\nu(\mathbf{U})V_{\nu+\Delta\nu}^*(\mathbf{U}) \rangle &= \frac{[\bar{I}_\nu \theta_0^2]^2}{2} \int_0^\infty dk_\parallel \frac{P_{\text{HI}}(k)}{r_\nu^2 \theta_0^2} \cos(k_\parallel r'_\nu \Delta\nu) \times \\ &\quad \times \left[1 + \beta \frac{k_\parallel^2}{k^2} \right]^2 \text{ with } k = \sqrt{k_\parallel^2 + (2\pi/r_\nu)^2 U^2} \end{aligned} \quad (13)$$

Equations (11) and (13) represent the main results of this section. They relate the correlation in the visibilities to the power spectrum of fluctuations in the HI distribution. The visibility correlations

at any baseline U are seen to be sensitive to Fourier modes $\geq 2\pi U/r_\nu$. It comes from the fact that each visibility measurement is sensitive to one Fourier mode in the plane of the sky, which arises from the projection of three-dimensional Fourier modes making different angles with the plane of the sky. The typical length scales $\simeq \pi/k$ that contribute to the measurement for any baseline U are $\lesssim 30h^{-1}$ Mpc($100/U$).

In the next section we use these equations to make predictions for the visibility correlations expected in the currently favoured cosmological models and we discuss the possibility of observing these.

3. Results

Equation (3) can be calculated to give:

$$\bar{I}_\nu = \frac{5.4 h \text{ Jy}}{\text{degree}^2} \Omega_{gas}(z) [\Omega_{m0}(1+z)^3 + \Omega_{\Lambda0}]^{1/2} (1+z)^{-3} \quad (14)$$

for a spatially flat cosmological model. Here $(1+z) = 1420/\nu$, ν being the observed frequency. We use $\Omega_{gas}(z) = 10^{-3}$ as a fiducial value throughout for $z \geq 1$ (Peroux *et al.* 2001). We give results for the currently-favoured cosmological model: spatially-flat with $\Omega_{\Lambda0} = 0.7$ and $\Omega_{m0} = 0.3$ (Perlmutter *et al.* 1999, de Bernardis *et al.* 2000). We use $h = 0.7$ whenever quoting a numerical value (Freedman *et al.* 2001).

For GMRT $\theta_{\text{FWHM}} = 1.8^\circ \times (325 \text{ MHz}/\nu)$. We plot the visibility correlation function in Figures 2 and 3 for the GMRT channels centered around $\nu = 325 \text{ MHz}$ and $\nu = 610 \text{ MHz}$ for COBE-normalized power spectrum (Bunn & White 1996) and $b = 1$. GMRT has a total bandwidth of 16 MHz at these frequencies in 128 channels. The visibility correlation function shown in the figures is averaged over one of the these channels with $\Delta\nu = 1.25 \text{ kHz}$. The correlation function is not very sensitive to the width of the channel so long as the channel width \lesssim a few kHz.

For $\nu = \nu'$, the signal $(\sqrt{\langle V_\nu(\mathbf{U})V_{\nu'}(\mathbf{U}) \rangle})$ is $10\text{--}50 \mu\text{Jy}$ for baselines $|\mathbf{U}| \simeq 100\text{--}1000$. GMRT has 15 antennas in a central array within a radius of $\simeq 1 \text{ km}$. Antenna pairs formed from these antennas will be most sensitive to the signal.

For $\nu \neq \nu'$, the correlation signal is seen to dip sharply as frequency separation is increased. The signal is anti-correlated and drops below $\simeq 1 \mu\text{Jy}$ for $\nu' - \nu \geq 2 \text{ MHz}$. For $\nu' - \nu \leq 0.5 \text{ MHz}$ the signal is $5\text{--}30 \mu\text{Jy}$ for baselines $\lesssim 500$.

In Figure 2 and 3 we assume that the HI distribution follows the underlying dark matter distribution, i.e. $b = 1$. However this may not be true; observed structures at any redshift are expected to be biased with respect to the underlying mass distribution (see e.g. Bardeen *et al.* 1986). This bias is expected to be higher at larger redshifts and the observed strong clustering of high redshift galaxies is at least partly owing to this fact (Steidel *et al.* 1998). In this paper we adopt a simple model of bias and assume it to be linear and independent of the Fourier mode.

Though the exact dependence of the HI signal on the bias is complicated (Eq. (13), the signal scales roughly linearly with bias. This means that for a moderately biased HI distribution $b \leq 2$ the signal could be higher by a factor of two.

4. Noise

For each visibility measurement in the UV plane, the contribution comes from both the signal from HI fluctuations S_ν , the detector noise N_ν , and various galactic and extragalactic foregrounds. We consider here the contribution from only the HI signal and the noise. The visibility measurement gives:

$$V_\nu(\mathbf{U}) = S_\nu(\mathbf{U}) + N_\nu(\mathbf{U}) \quad (15)$$

Both S and N are complex quantities with both real and imaginary parts distributed as Gaussian random variables (see e.g. Crane & Napier 1989 for properties of noise). The signal is a Gaussian random field because it is linear in density perturbation $\Delta(\vec{k})$ which is expected to be a Gaussian random field for large scales (small k) (see e.g. Peacock 1999, Bardeen *et al.* 1986). The signal and noise are uncorrelated with each other. The reality condition of the surface brightness (Eq. 1) and the noise in the real space implies $S(-\mathbf{U}) = S^*(\mathbf{U})$ and $N(-\mathbf{U}) = N^*(\mathbf{U})$. Our aim is to construct bilinear combinations like $V_\nu(\mathbf{U})V_{\nu'}^*(\mathbf{U})$ and to detect $S_\nu(\mathbf{U})S_{\nu'}^*(\mathbf{U})$. ν and ν' will in general be different. The average signal $\langle S_\nu(\mathbf{U})S_{\nu'}^*(\mathbf{U}) \rangle$ is calculated in the previous section. The average noise correlation, for $\nu = \nu'$:

$$\langle N_\nu(\mathbf{U})N_\nu^*(\mathbf{U}) \rangle = \left[\frac{T_{\text{sys}}}{K\sqrt{\Delta\nu\Delta t}} \right]^2 \quad (16)$$

Here T_{sys} is the system temperature, $\Delta\nu$ is the bandwidth, K is the antenna gain, and Δt is the time of integration for one visibility measurement. For $\nu \neq \nu'$ the noise correlation vanishes as the noise in different frequency channels is uncorrelated.

Estimator of the signal: From the measured visibility it is possible to write several estimators of the signal. The simplest such estimator is:

$$\hat{S} = V_\nu(\mathbf{U})V_{\nu'}^*(\mathbf{U}) - \langle N_\nu(\mathbf{U})N_{\nu'}^*(\mathbf{U}) \rangle \quad (17)$$

This estimator is clearly unbiased, i.e.

$$\langle \hat{S} \rangle = \langle S_\nu(\mathbf{U})S_{\nu'}^*(\mathbf{U}) \rangle.$$

The quantity of interest to us is the variance of the estimated signal: $\sigma(\hat{S})^2 = \langle \hat{S}^2 \rangle - \langle \hat{S} \rangle^2$. This quantity is calculated to be (see Appendix A for a derivation):

$$\sigma^2(\hat{S}) \simeq \frac{q}{n} \langle N_\nu(\mathbf{U})N_\nu^*(\mathbf{U}) \rangle^2 \quad (18)$$

$q = 2$ for $\nu = \nu'$ and $q = 1$ for $\nu \neq \nu'$. n is the total number of visibility measurements. The signal-to-noise for the detection of the HI fluctuation signal is $\langle \hat{S} \rangle / \sigma(\hat{S})$.

The value of n for a given $|\mathbf{U}|$ in general depends on the antenna positions, frequency coverage, and the position of the source in the sky. To calculate the value of n we first consider the case when $\nu = \nu'$.

Case I– $\nu = \nu'$: To get a simple estimate, assume that a pair of antennas describes circular tracks in the UV plane with radius $|\mathbf{U}|$ and that these tracks do not overlap with the tracks of other antenna pairs, then $n = T/\Delta t$ for each frequency channel, where T is the total time of observation. (The actual observation is more complicated because the antenna tracks cross in the UV plane.) For this case, Eq. (18) gives, using Eq. (16):

$$\sigma^2(\hat{S}) = \left[\frac{2T_{\text{sys}}}{K\sqrt{\Delta\nu T}} \right]^2 \quad (19)$$

Before proceeding further it is useful to calculate the expected noise for the GMRT. We shall take the fiducial observing frequency to be $\simeq 320$ MHz. At this frequency the GMRT system temperature $T_s \simeq 110$ K. GMRT has a total bandwidth of 16 MHz at this frequency in 128 channels. To calculate the quantity in Eq. (16) we take one channel ($\Delta\nu = 125$ kHz) and an integration time of $\Delta t = 30$ sec for one 'instantaneous' measurement for a given baseline. The antenna gain at this frequency $K = 0.32$ K Jy $^{-1}$. Using this Eq. (16) gives the noise correlation to be $\simeq 175$ mJy. As this is much larger than the expected signal calculated in the last section, we are justified in neglecting the signal term in Eq. (26) in the appendix. For total time of integration $T = 10$ hrs, Eq. (19) gives $\sigma(\hat{S}) \simeq 5$ mJy.

As each frequency channel gives a realization of the signal, the noise can be reduced further by using all the frequency channels. This gives $n = N_{\text{chan}} \times T/\Delta t$ with $N_{\text{chan}} = 128$ for GMRT; Eq. (19) gives $\sigma(\hat{S}) \simeq 0.45$ mJy. Even though we made a few simplifying assumptions in calculating the noise, this is the typical value obtainable in a real experiment. The expected noise is much larger than the expected signal from the HI fluctuations and therefore an experiment like GMRT cannot detect the HI fluctuation for a given $|\mathbf{U}|$ or by using a single pair of antennas in a reasonable amount of integration time.

To reduce the noise further one must consider averaging the signal over more than one pair of antennas. One such estimator is the map RMS which uses information from all possible baselines. The total number of 'instantaneous' baselines for an experiment with N antennas is $N(N - 1)/2$. This gives $n = N_{\text{chan}}N(N - 1)/2 \times T/\Delta t$ and gives a further decrease of a factor $\simeq N/\sqrt{2}$ in the sensitivity. In the previous section we showed that much of the contribution to signal comes from baselines $\leq 1000\lambda$. GMRT has 15 antennas in the central array within a radius of $\simeq 1$ km. Much of the contribution to the signal will come from these antenna pairs.

Taking $N = 15$ in the calculation of noise sensitivity, we get $\sigma(\hat{S}) \simeq 40$ μ Jy for 10 hours of integration. The average signal (averaged over 15 antennas of the central GMRT array) is $\simeq 20$ – 40 μ Jy. This means that a few sigma detection of the signal might be feasible in integration time ≤ 100 hrs using the central array of GMRT.

Case II– $\nu \neq \nu'$: In this case, $\langle N_\nu(\mathbf{U})N_\nu^*(\mathbf{U}) \rangle = 0$ and the variance of the signal estimator

is smaller by a factor of 2 (Eq. (18)). The rest of the calculations proceeds similar to the first case. The number of distinct pairs for two different frequencies will depend on the separation of the frequencies. However, one must also take into account the line width of the damped Lyman- α clouds which is $\simeq 200 \text{ km sec}^{-1}$ (Prochaska & Wolfe 1998). The line width of each GMRT channel is $\simeq 120 \text{ km sec}^{-1}$. This means that one damped Lyman- α cloud will spill over in many frequency channels, thereby creating a correlation in the signal for nearby channels. This correlation must be accounted for before the HI fluctuation signal can be extracted. It is hard to do it analytically and this issue will be addressed in future using simulations of the HI signal. However it is possible to get the typical noise sensitivity for this measurement.

The total number of frequency channel pairs is $N_{\text{chan}}(N_{\text{chan}} - 1)/2$. Each pair gives a different realization of noise. If we average the signal over all baselines and all frequency pairs, we get $n = N(N - 1)/2N_{\text{chan}}(N_{\text{chan}} - 1)/2$. This is larger than the maximum value of n in the first case by a factor of $\simeq N_{\text{chan}}/2$. However it would be meaningful to average over all channel-pairs if the signal is significant for all such cross-correlations. As seen in the previous section, the correlation between different channels falls rapidly for separation $\geq 1 \text{ MHz}$, therefore the number of useful channels pairs is less than the maximum possible. The value of n however is still likely to be more than in the previous case. For example if we average the signal over all the frequency channels with $\nu' - \nu \leq 0.5 \text{ MHz}$, the expected signal is $\simeq 10\text{--}20 \mu\text{Jy}$. The number of frequency pairs are $\simeq 5N_{\text{chan}}$ in this case. This gives $\sigma(\hat{S}) \simeq 15 \mu\text{Jy}$ for ten hours of integration. From this discussion we can conclude that it might also be possible to extract this signal for integration time $\leq 100 \text{ hrs}$ using GMRT.

The noise in detecting the HI signal $\sigma(\hat{S})$ is comparable to the sensitivity for detecting continuum sources. This is so even though the HI clouds emit line radiation. Therefore the method of observing fluctuations in HI radiation makes more optimal use of all the frequency width available in the experiment. The individual clouds are very faint (flux $\lesssim 10 \mu\text{Jy}$ (Saini *et al.* 2001)) and cannot be detected using GMRT because the line sensitivity $\simeq 50 \mu\text{Jy}$ for 100 hrs of integration needed to detect the HI fluctuations.

5. Conclusions and Discussion

Our main results are:

1. The correlation in measured visibilities owing to density inhomogeneities and peculiar velocities of the HI distribution at high redshifts can be related to the power spectrum of the HI distribution (Eq. (13)). The visibility correlation for any baseline U is sensitive to Fourier modes $\geq 2\pi U/r_\nu$. This means that the typical length scales probed for any baseline are $\lesssim 30h^{-1} \text{ Mpc}(100/U)$.
2. The signal is strongest for baselines $\lesssim 1000$ and for $\nu = \nu'$, i.e. on the same two-dimensional

map, the correlation is between 2×10^{-9} Jy 2 and 10^{-10} Jy 2 .

3. For $\nu \neq \nu'$, i.e., cross-correlation signal, the correlation signal is 10^{-9} – 10^{-11} Jy 2 for baselines $|\mathbf{U}| \lesssim 500$ for $\nu' - \nu \lesssim 0.5$ MHz. The correlation is negative for most baselines for $\nu' - \nu \gtrsim 2$ MHz and falls below 10^{-12} Jy 2 .
4. GMRT might detect these signals for integration times $\lesssim 100$ hrs. We argue that measuring visibility correlations in the presence of system noise makes optimal use of the fact that the noise is uncorrelated across baselines and frequency channels. The error for these measurements is comparable to and can even be smaller than the continuum sensitivity of the instrument.

The signal and noise analyses given in this paper are for the system parameters of the currently-operational GMRT. However it can be easily extended to future telescopes like Square Kilometer Array (SKA)¹ and Low Frequency Array (LOFAR)². Our analysis can also be extended to higher redshifts ($z \simeq 5$) as the HI content of the universe at these redshifts is beginning to be known (see e.g. Peroux *et al.* 2001).

In this paper we neglected two other contributions to the visibility correlations: galactic and extra-galactic foregrounds and the Poisson fluctuations owing to point-like nature of HI clouds. The galactic foregrounds are expected to be dominated by the fluctuations in the synchrotron radiation from the Galaxy. The only existing all-sky map at low radio frequencies is the 408 MHz Haslam map (Haslam *et al.* 1982). This map has an angular resolution of $\simeq 1^\circ$ and therefore cannot give much information on the angular scales of interest to us. The extra-galactic foregrounds get most of its contribution from the radio point-sources. Little is known about the radio point sources at sensitivity levels ($\lesssim 100 \mu\text{Jy}$) and frequencies of relevance in this paper. However it seems likely that these foregrounds will dominate the HI signal (BNS 2001), and a possible strategy to remove foregrounds was discussed in BNS (2001). This issue will be discussed in a later paper by using simulations of the HI signal and the foregrounds.

The HI at large redshift is locked up in discrete clouds. This will give rise to visibility correlations even in the absence of gravitational instability. This signal also depends on the mass function of the HI clouds (Saini *et al.* 2001) and therefore the detection of this signal can give important clue about how the HI at high redshift is distributed. We shall attempt to estimate this signal from simulation of the high redshift HI in a later publication.

¹see <http://www.nfra.nl/skai/>

²see <http://www.astron.nl/lofar>

Acknowledgements

The authors would like to thank Jayaram Chengalur for many useful discussions. We are thankful to late K. R. Anantharamiah for helpful comments on the noise properties of interferometric experiments.

Appendix A

The HI fluctuation signal and the noise satisfy the following conditions:

$$\langle S_\nu(\mathbf{U})S_{\nu'}(\mathbf{U}') \rangle = \langle S_\nu(\mathbf{U})S_{\nu'}(\mathbf{U}) \rangle \delta_D(\mathbf{U} - \mathbf{U}') \quad (20)$$

$$\langle N_\nu(\mathbf{U})N_{\nu'}(\mathbf{U}') \rangle = \langle N_\nu(\mathbf{U})N_{\nu'}(\mathbf{U}) \rangle \delta_D(\mathbf{U} - \mathbf{U}') \delta_D(\nu - \nu') \quad (21)$$

Note that the signal is correlated across frequency channels while the noise is not. Let us assume that any interferometric experiment makes n measurements of the visibility for given $|\mathbf{U}|$ and the quantities (like visibility correlation function) are estimated by averaging over these measurement. Using this it is seen that the signal (for $\nu = \nu'$) and the noise can be treated as n uncorrelated, random variables with the same mean and variance. In such a case, the estimated average equals the average of any of the random numbers and the variance of the estimated 'signal' is $1/n$ times the variance of any of the random variable (see e.g. Papoulis 1965; this result is independent of the probability distribution functions of the individual variables). Of particular interest to us is the variance of the estimator in Eq. (17) for a given $|\vec{u}|$. The variance is estimated from n realizations of the random variable \hat{S} . It is given by:

$$\sigma^2(\hat{S}) = \frac{\sigma^2}{n} \quad (22)$$

Here $\sigma^2 = \langle \hat{S}^2 \rangle - \langle \hat{S} \rangle^2$ is the variance of any realization of \hat{S} .

It is given by, using the definitions of V and N from Eq. (15):

$$\sigma^2 = \langle V_\nu V_{\nu'} V_{\nu'} V_\nu \rangle + \langle N_\nu N_{\nu'} \rangle^2 - 2\langle N_\nu N_{\nu'} \rangle \langle V_\nu V_{\nu'} \rangle - \langle S_\nu S_{\nu'} \rangle^2 \quad (23)$$

To simplify this expression further we use the fact that for a Gaussian random process, the expectation value of four random numbers is given by

$$\langle x_1 x_2 x_3 x_4 \rangle = \langle x_1 x_2 \rangle \langle x_3 x_4 \rangle + \langle x_1 x_3 \rangle \langle x_2 x_4 \rangle + \langle x_2 x_4 \rangle \langle x_1 x_3 \rangle$$

We first consider the case when $\nu = \nu'$. Eq. (23) then reduces to:

$$\sigma^2 = 3\langle V_\nu V_{\nu'} \rangle^2 + \langle N_\nu N_{\nu'} \rangle^2 - 2\langle N_\nu N_{\nu'} \rangle \langle V_\nu V_{\nu'} \rangle - \langle S_\nu S_{\nu'} \rangle^2 \quad (24)$$

Again using Eq. (15) for the definition of $\langle V_\nu V_{\nu'} \rangle$, this simplifies to:

$$\sigma^2 = 2 \times (\langle S_\nu S_\nu \rangle + \langle N_\nu N_\nu \rangle)^2 \quad (25)$$

The case when $\nu = \nu'$ is slightly more complicated. Making a simplifying assumption that the signal contribution can be dropped while calculating the four-point functions in Eq. (23) (for justification see the text), we get:

$$\sigma^2 \simeq \langle N_\nu N_\nu \rangle^2 \quad (26)$$

Eqs. (25) and (26) along with Eq. (22) gives Eq. (18).

REFERENCES

- Bagla, J. S. 1999, ASP Conf. Ser. 156: Highly Redshifted Radio Lines, 9
- Bagla, J.S., Nath, B. and Padmanabhan, T. 1997, MNRAS, 289, 671
- Bharadwaj, S., Nath, B. & Sethi, S. 2001, JAA, 22, 21
- Bardeen, J. M., Bond, J. R., Kaiser, N., & Szalay, A. S. 1986, ApJ, 304, 1
- Bunn E. F. & White M. 1996, ApJ, 460, 1071
- Crane, P. C. & Napier, P. J. 1989, in *Synthesis Imaging in Radio Astronomy*, ASP series, volume 6
- de Bernardis, P. *et al.* 2000, Nature, 404, 995
- Freedman, W. *et al.* 2001, ApJ, 553, 47
- Haslam, C. G. T., Stoffel, H. , Salter, C. J. & Wilson, W. E. 1982, ApJS, 47, 1
- Kumar A., Padmanabhan T. and Subramanian K. 1995, MNRAS, 272, 544
- Lahav O., Lilje P. B., Primack J. R. and Rees M., 1991, MNRAS, 251, 128
- Lanzetta, K. M., Wolfe, A. M., Turnshek, D. A. 1995, ApJ, 430, 435
- Papoulis, A. 1984, *Probability, Random Variables, and Stochastic Processes*, McGraw-Hill
- Peacock, J. A. 1999, *Cosmological Physics* , Cambridge, Cambridge University Press
- Peebles, P. J. E. 1980, *The Large-Scale Structure of the Universe* , Princeton, Princeton University Press
- Perlmutter, S. *et al.* 1999, ApJ, 517, 565
- Péroux, C., McMahon, R. G., Storrie-Lombardi, L. J. & Irwin, M .J. 2001, MNRAS
- Prochaska, J. X. & Wolfe, A. M. 1998, ApJ, 507, 113
- Saini, T., Bharadwaj, S. & Sethi, S. 2001, ApJ, 557, 421

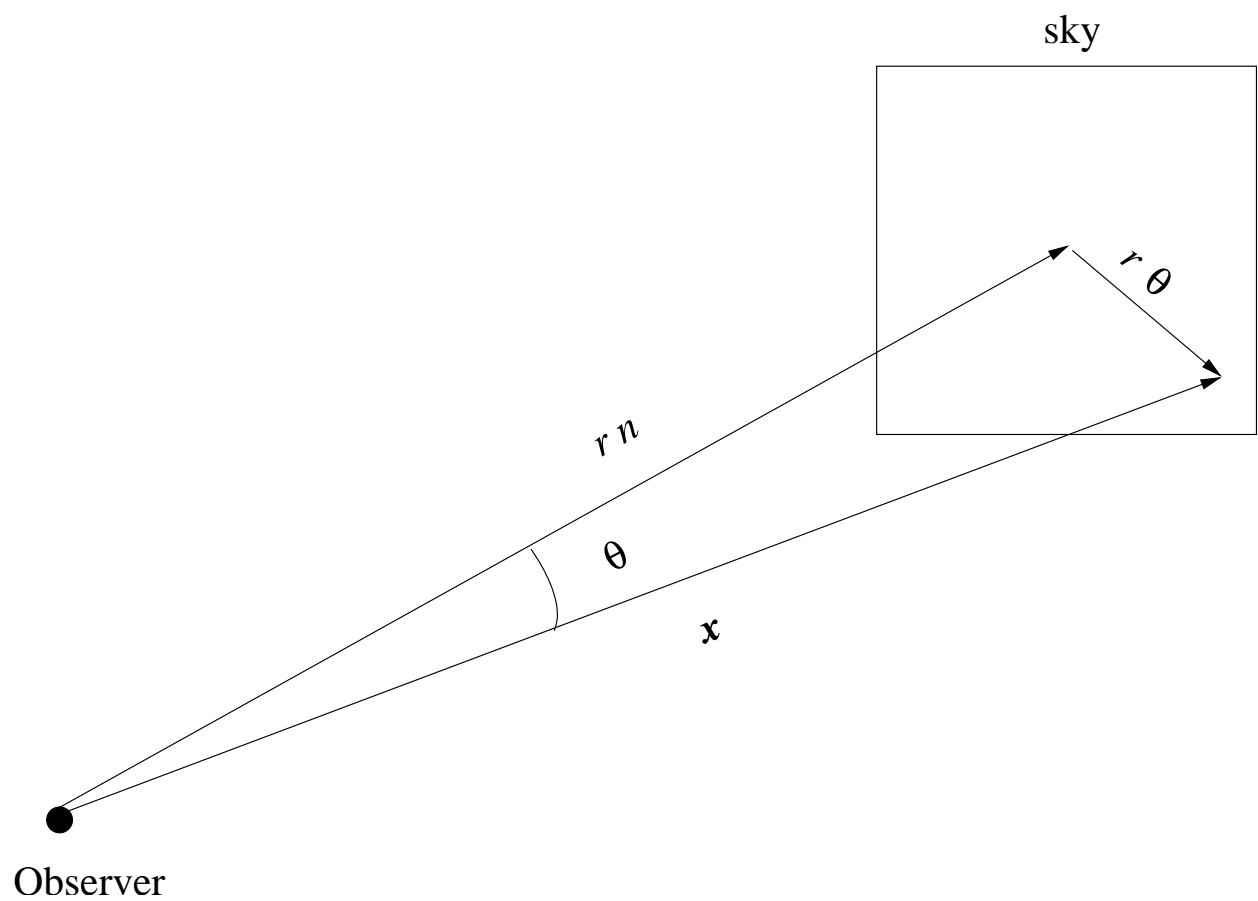
Steidel, C. *et al.* 1998, ApJ, 492, 428

Storrie–Lombardi, L.J., McMahon, R.G., Irwin, M.J. 1996, MNRAS, 283, L79

Subramanian, K. and Padmanabhan, T. 1993, MNRAS, 265, 101

Subrahmanyam. R. & Anantharamaiah, K. R. JAA, 1990, 11, 221:

Swarup, G., Ananthakrishnan, S., Kapahi, V. K., Rao, A. P., Subrahmanya, C. R., & Kulkarni, V. K. 1991, Curr. Sci., 60, 95



Observer

Fig. 1.— The geometry for the flat-sky approximation is shown.

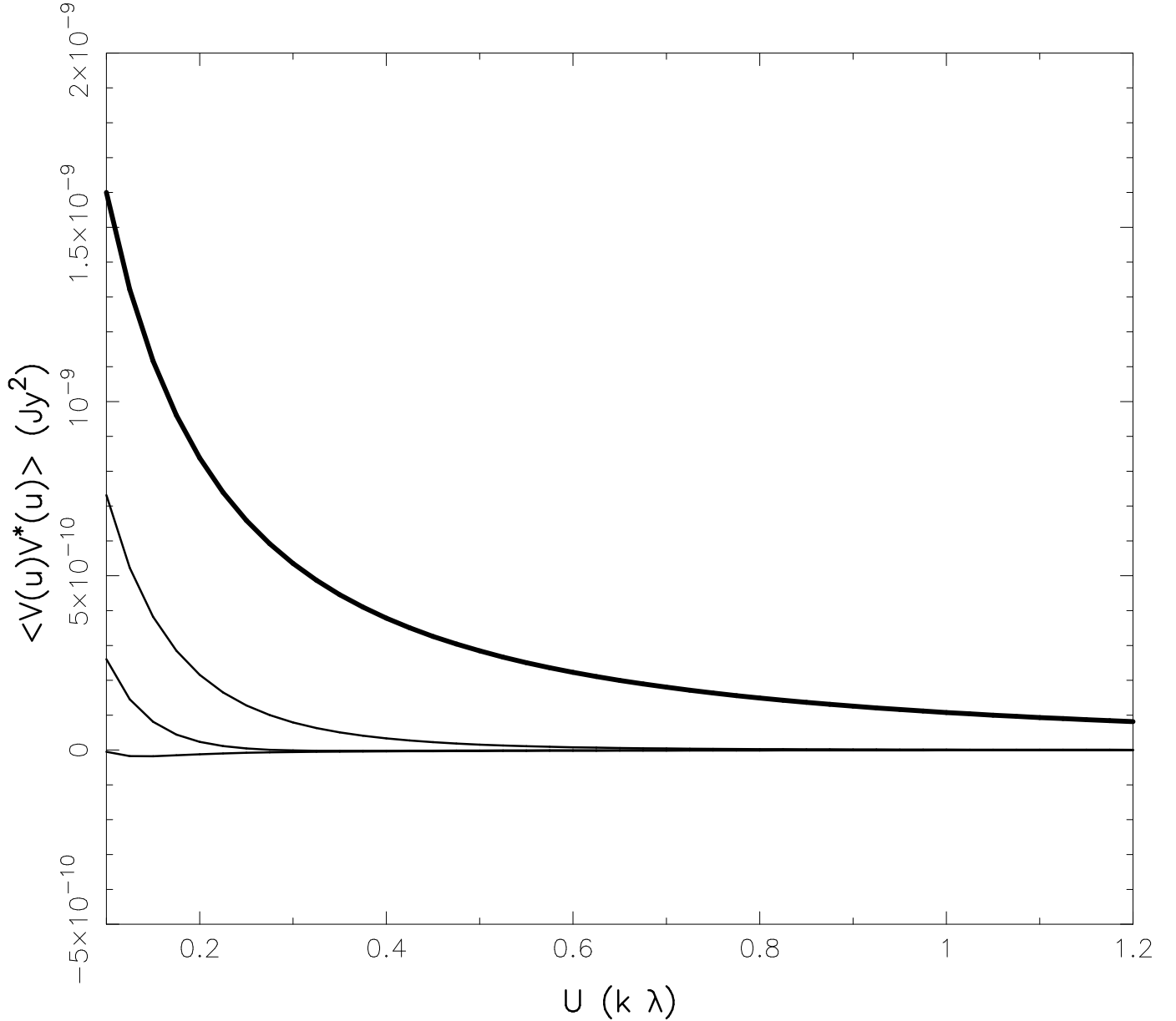


Fig. 2.— For the central frequency $\nu = 320$ MHz, this figure shows the visibility correlation function as baseline U varies. The thick curve shows the visibility correlation for $\nu = \nu'$. The other three curves show, from top to bottom, the visibility correlation for $\nu' - \nu = \{0.5, 1, 2\}$ MHz, respectively.

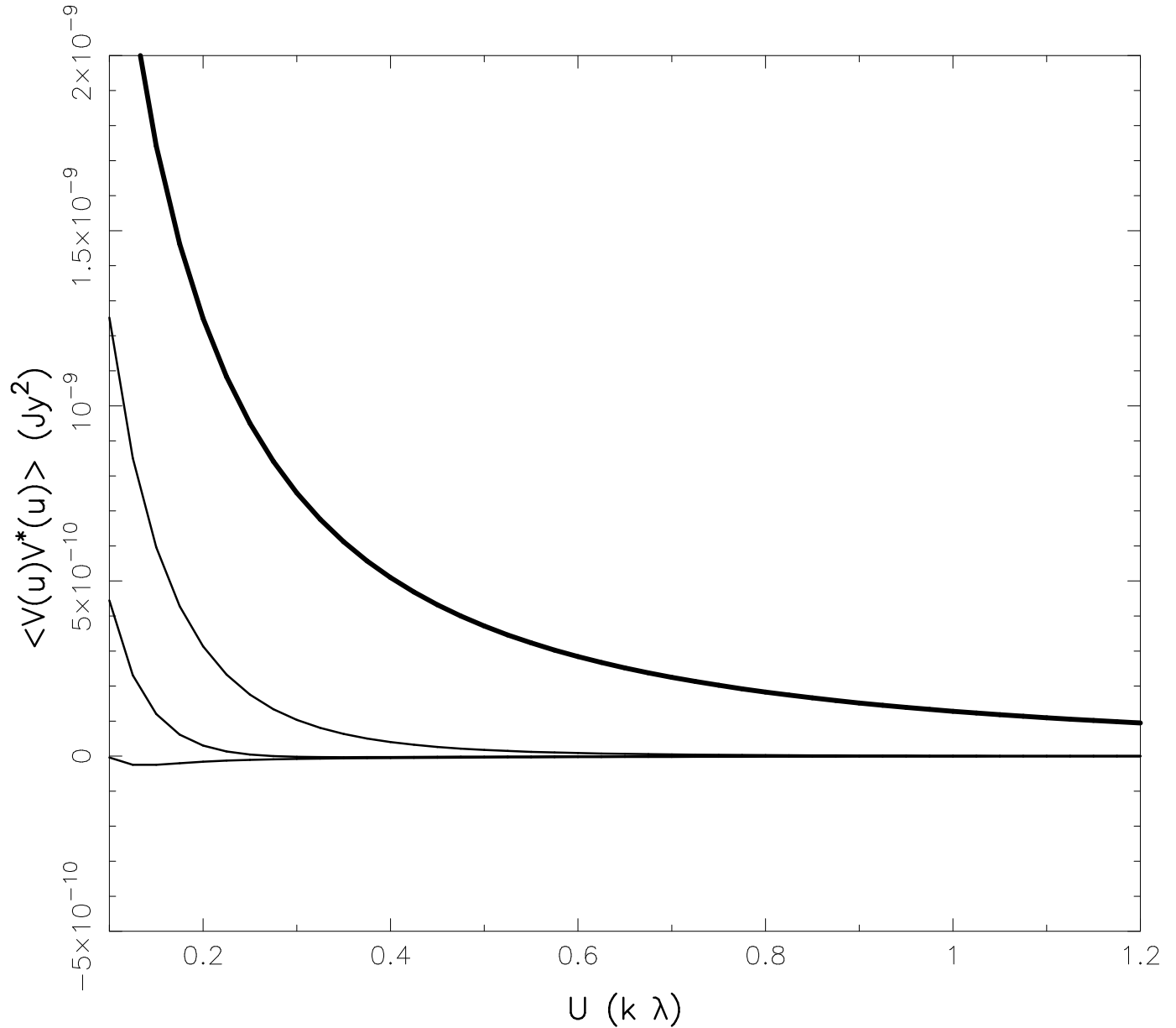


Fig. 3.— Same as Figure 2 for the central frequency $\nu = 610$ MHz